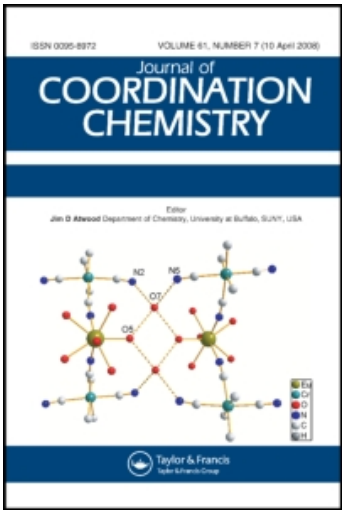

Journal of Coordination Chemistry
Publication details, including instructions for authors and subscription information:
http://www.informaworld.com/smpp/title~content=t713455674

Syntheses, crystal structures and magnetic properties of heteronuclear bimetallic compounds of $[Cu(pdc)_2][M(H_2O)_5]\cdot 2H_2O$ [M=Ni(II), Co(II), Mn(II); pdc=2,6-pyridinedicarboxylato]

Alexander R. Parent[a]; Srikanth Vedachalam[a]; Christopher P. Landee[b]; Mark M. Turnbull[a]
[a] Carlson School of Chemistry and Biochemistry, [b] Dept. of Physics, Clark University, Worcester, MA 01610, USA

To cite this Article Parent, Alexander R. , Vedachalam, Srikanth , Landee, Christopher P. and Turnbull, Mark M.(2008) 'Syntheses, crystal structures and magnetic properties of heteronuclear bimetallic compounds of $[Cu(pdc)_2][M(H_2O)_5]\cdot 2H_2O$ [M=Ni(II), Co(II), Mn(II); pdc=2,6-pyridinedicarboxylato]', Journal of Coordination Chemistry, 61: 1, 93 — 108
To link to this Article: DOI: 10.1080/00958970701732808
URL: http://dx.doi.org/10.1080/00958970701732808

Journal of Coordination Chemistry
Vol. 61, No. 1, 10 January 2008, 93–108

Taylor & Francis
Taylor & Francis Group

Syntheses, crystal structures and magnetic properties of heteronuclear bimetallic compounds of $[Cu(pdc)_2][M(H_2O)_5]\cdot 2H_2O$ [M = Ni(II), Co(II), Mn(II); pdc = 2,6-pyridinedicarboxylato]

ALEXANDER R. PARENT†, SRIKANTH VEDACHALAM†, CHRISTOPHER P. LANDEE‡ and MARK M. TURNBULL*†

†Carlson School of Chemistry and Biochemistry
‡Dept. of Physics, Clark University, Worcester, MA 01610 USA

(*Received 12 June 2007; in final form 21 September 2007*)

The complexes $[M(H_2O)_5][Cu(pdc)_2]\cdot 2H_2O$ [M = Ni(II) **1**, Co(II) **2**, Mn(II) **3**; pcd = 2,6-pyridinedicarboxylato] are prepared and their crystal structures, magnetic susceptibilities and UV-Visible properties reported. In all cases, the Cu(II) ion occupies the chelating site in the pdc ligand, while the M(II) occurs as a pentaaqua ion bridged to the $[Cu(pdc)_2]$ moiety through a carboxylate as demonstrated by both UV-Visible spectroscopy and X-ray diffraction. Single crystal X-ray diffraction shows the three complexes to be isostructural. Weak antiferromagnetic interactions between the metal ions are observed in **1** and **3**, while the magnetic behavior of **2** is dominated by single ion anisotropy.

Keywords: Copper(II); Manganese(II); Nickel(II); Cobalt(II); Pyridinedicarboxylate; Crystal structure; Magnetic properties; Bimetallics; Dipicolinate

1. Introduction

Our group is involved in the crystallographic and magnetic characterization of various metal ligand coordination networks [1]. These networks can consist of one-, two-, or three-dimensional lattices, or, as in the title compounds, as isolated dimers in the solid state. Dimers can be especially interesting for study because the high degree of isolation around the metal centers greatly reduces the complexity of calculations necessary to model the magnetic properties, thus allowing for a more detailed study of complex phenomena. Heteronuclear bimetallic species are themselves extremely interesting compounds, and such species have been found to demonstrate ferrimagnetism [2], in which adjacent metal centers couple in an antiferromagnetic fashion, yet have a net moment at low temperature due to incomplete quenching, and hysteresis [3] in one and higher dimensional species. Although ferrimagnetism cannot occur without the long

*Corresponding author. Email: Mturnbull@clarku.edu

ISSN 0095-8972 print/ISSN 1029-0389 online © 2008 Taylor & Francis
DOI: 10.1080/00958970701732808

range ordering found in higher dimensional networks, dimeric heteronuclear species have also been shown to exhibit hysteresis and the incomplete quenching of moments prerequisite for ferrimagnetism [4]. 2,6-Pyridinedicarboxylic acid (pdca) has been used to produce homonuclear dimeric species of Cu [5], Ni [6], and Mn [7] with great success. The 2,6-pyridinedicarboxylato (pdc) ligand has been well characterized [8, 9] and magnetic data has been obtained for two polymorphs of the $[Cu(pdc)(H_2O)_2]$ 1-D chain [8b,c]. The excellent results obtained by these experiments led us to attempt to synthesize heteronuclear dimeric species using pdc. We report here the synthesis, structure and magnetic properties of $[M(H_2O)_5][Cu(pdc)_2] \cdot 2H_2O$ [M = Ni(II), Co(II), Mn(II)]. A recent article has reported the synthesis of several compounds of the formula $[M(H_2O)_5][M'(pdc)_2] \cdot 2H_2O$ (M = Cu; M′ = Ni, Co, Zn; M = Zn; M′ = Co; M = Ni, M′ = Co) [10]. Although our experimental results are consistent with their reported data, we are unable to support their assignment of the metal centers for the title compounds.

2. Experimental

2,6-Pyridinedicarboxylic acid was purchased from Aldrich Chemical Company and used without further purification. NaOH was purchased from EMD Chemicals and used without further purification. The transition metal nitrates were obtained as follows: $Co(NO_3)_2 \cdot 6H_2O$, $Cu(NO_3)_2 \cdot 3H_2O$, Mallinckrodt Chemical Company; $Mn(NO_3)_2$ (aq.) Fisher Scientific Company; $Ni(NO_3)_2 \cdot 6H_2O$ J.T. Baker Chemical Company. IR spectra were recorded on a Perkin-Elmer 1600 spectrophotometer and referenced to polystyrene. UV-Visible data were recorded on a Perkin-Elmer Lambda 40 spectrometer and referenced to water.

2.1. *Pentaaquanickel(II)*bis-*2,6-pyridinedicarboxalatocuprate(II)dihydrate (1)*

2,6-Pyridinedicarboxylic acid (1.669 g, 9.99 mmol) (pdca) was combined with NaOH (0.799 g, 20.0 mmol) in 50 mL of water. An additional 0.02 g (0.5 mmol) of NaOH was required to achieve complete dissolution of the pdca. A solution of $Cu(NO_3)_2 \cdot 3H_2O$ (1.246 g, 5.14 mmol) in 26 mL of water was then added to the pdc solution. A solution of $Ni(NO_3)_2 \cdot 6H_2O$ (1.467 g, 5.04 mmol) in 31 mL of water was added to the Cu-pdc solution. The solution was left at room temperature to evaporate. After one day small green crystals began to form. The crystals were recovered by vacuum filtration after three days (0.567 g, 19%). An additional 0.385 g (13%) of product was harvested after an additional five days. M.p. 98–102°C (d). Anal. Calcd for $C_{14}H_{20}N_2O_{15}NiCu$ (found) – C 29.06 (28.91); H 3.49 (3.71); N 4.84 (4.36). Vis: 773 nm, $\varepsilon = 64\ M^{-1}cm^{-1}$ ($Cu(pdc)_2^{2-}$). IR (KBr): 3524 m, 3200 s/br, 1648 m, 1618 s, 1578 s, 1560 m, 1542 m, 1434 m, 1386 s, 1283 m.

2.2. *Pentaaquacobalt(II)*bis-*2,6-pyridinedicarboxalatocuprate(II)dihydrate (2)*

2,6-Pyridinedicarboxylic acid (1.671 g 10.0 mmol) (pdca) was combined with NaOH (0.800 g, 20.0 mmol) and dissolved in 51 mL of water. A solution of $Cu(NO_3)_2 \cdot 3H_2O$

(1.248 g, 5.17 mmol) in 43 mL of water was then added to the pdc solution. A solution of $Co(NO_3)_2 \cdot 6H_2O$ (1.474 g, 5.04 mmol) in 43 mL of water was then added to the Cu-pdc solution. A lavender precipitate immediately formed, and an additional 180 mL of water and 1 mL of 2N nitric acid were added to the solution to dissolve the precipitate. The solution was then warmed slightly and left to evaporate. After one day dichroic crystals (purple-red/lavender) began to appear in solution. The crystals were isolated by vacuum filtration, washed with cold water and air-dried (0.836 g, 29%). Additional product was collected using the same procedure after 8 and 10 days further evaporation of the filtrate. Total recovery: 1.134 g (39%). M.p. 99–100°C (d). Anal. Calcd for $C_{14}H_{20}N_2O_{15}CoCu$ (found) – C 29.00 (28.86); H 3.48 (3.82); N 4.83 (4.39). Vis: 778 nm, $\varepsilon = 61\ M^{-1}cm^{-1}$ ($Cu(pdc)_2^{2-}$), 514 nm $8.0\ M^{-1}cm^{-1}$ ($Co(H_2O)_6^{2+}$). IR (KBr): 3529 m/br, 3216 s/br, 1671 m, 1618 s, 1578 s, 1434 m, 1384 s, 1282 m cm^{-1}.

2.3. *Pentaaquamanganese(II)*bis-*2,6-pyridinedicarboxalatocuprate(II)dihydrate (3)*

2,6-Pyridinedicarboxylic acid (1.667 g, 9.98 mmol), (pdca) was combined with NaOH (0.795 g, 19.9 mmol) and dissolved in 50 mL of water. A solution of $Cu(NO_3)_2 \cdot 3H_2O$ (1.241 g, 5.13 mmol) in 30 mL of water was then added to the pdc solution. A solution of 50 wt.% of $Mn(NO_3)_2$ in water (1.809 g, 5.02 mmol) was then added to the Cu-pdc solution. A light blue precipitate formed immediately. An additional 82 mL of water and 9 drops of 2 N nitric acid were added to dissolve the precipitate. The solution was then left at room temperature to evaporate. After four days, 0.871 g (30%) of aqua colored crystals were collected via vacuum filtration. An additional 0.152 g (5.3%) of crystals was collected from further evaporation of the filtrate after six days. M.p. 95-100°C (d). Anal. Calcd for $C_{14}H_{20}N_2O_{15}MnCu$ (found) – C 29.25 (29.02); H 3.51 (3.80); N 4.87 (4.51). Vis: 774 nm, $\varepsilon = 70\ M^{-1}cm^{-1}$ ($Cu(pdc)_2^{2-}$). IR (KBr): 3570 m, 3369 s/br, 3099 m, 1618 s, 1582 s, 1427 m, 1384 s, 1281 m, 1086 m cm^{-1}.

2.4. *UV-Vis characterization*

Solutions of $[Cu(H_2O)_6](NO_3)_2$ (2.0 mM), $[Ni(H_2O)_6](NO_3)_2$ (2.2mM), and $[Co(H_2O)_6](NO_3)_2$ (2.2 mM) were prepared by dissolving the metal nitrates in water. A solution of ($Cu(pdc)_2^{2-}$) (0.20 mM) was prepared by dissolving copper nitrate in a solution containing nine equivalents of Na_2pdc in water. Solutions of $Ni(pdc)_2^{2-}$ (0.44 mM) and ($Cu(pdc)_2^{2-}$) (0.44 mM) were prepared by dissolving the metal nitrates in solutions containing a four-fold molar excess of pdc in water. Solutions of **1** (3.4 mM), **2** (3.8 mM), and **3** (0.5 mM) were prepared by dissolving the crystalline product in water. Measurements were taken from 400 to 900 nm (300 to 900 nm for $[Ni(H_2O)_6](NO_3)_2$ due to a peak near 400 nm).

2.5. *X-ray structure determination*

Data collections for **1** and **2** were carried out on a Siemens P4 diffractometer employing Mo-Kα radiation ($\lambda = 0.71073$) and a graphite monochromator. Data collection via ω-scans, cell refinement and data reduction for **1** and **2** were performed

using SHELXTL (VMS) software [11]. Absorption corrections were made via ψ-scans. Data collection via φ and ω-scans, cell refinement and data reduction for **3** were performed by using a Bruker SMART system with a CCD area detector [12]. Absorption corrections for **1** were performed using SADABS [13]. For **2**, absorption corrections were calculated based on refined ΔF values. No absorption correction was made for **3**. The structures were solved using the heavy atom Patterson method [SHELXS-97] and full-matrix least-squares refinement was done via SHELXL-97 [14]. The aromatic hydrogen atoms were refined via a riding model with fixed isotropic U's. Hydrogen atoms bonded to water oxygen atoms were located in the difference map and their positions allowed to refine with fixed isotropic U's. In compounds **1** and **2a** residual peak in the difference map suggested the presence of a partial occupancy water molecule. Refinement showed 0.2 waters for **1** and 0.3 waters for **2**. The partial occupancy water molecules were not included in the final refinement. Neutral scattering factors and anomalous dispersion corrections for non-hydrogen atoms were taken from Ibers and Hamilton [15]. Crystallographic data may be found in table 1. Selected bond lengths and angles are given in table 2. Further data is listed in the supplementary Material [16].

2.6. *Magnetic susceptibility measurements*

Magnetic susceptibility was measured on a Quantum Design MPMS-XL SQUID magnetometer. Samples of single crystals were ground into fine powders and loaded in gelatin capsules. The moment of the samples was then measured at 1.8 K in a field varying from 0 to 50000 Oe; several data points were collected as the field returned to 0 Oe to check for hysteresis effects. In the case of **2** hysteresis was observed and an additional measurement of moment was made on the sample from 0 to 50000 to −50000 to 50000 Oe to characterize the effect. Temperature dependent magnetization was measured on each of the samples from 1.8 to 325 K in a 1 kOe field. The background contribution from the gelatin capsule was measured separately and subtracted from the data sets. Data were corrected for temperature independent paramagnetism and intrinsic diamagnetism using Pascal's constants.

3. Results

Reaction of 2,6-pyridinedicarboxylic acid, pdca, with NaOH followed by the addition of $Cu(NO_3)_2 \cdot 3H_2O$ and $M(NO_3)_2 \cdot xH_2O$ yielded $[M(H_2O)_5]$ $[Cu(pdc)_2] \cdot H_2O$ (scheme 1) [M = Ni (**1**); M = Co (**2**); M = Mn, x = 2 (**3**)] in yields ranging from 32–68% (see scheme 1). Single crystals suitable for X-ray diffraction were isolated for each compound and their structures were determined.

3.1. *Crystal structure analysis*

Compounds **1** and **2** crystallize in the triclinic $P\bar{1}$ space group, while **3** crystallized in the monoclinic $P2_1/c$ space group; complete crystallographic data may be found in table 1. Despite the different space groups, the three compounds are nearly isostructural,

Table 1. X-ray data for compounds **1**–**3**.

	1	**2**	**3**
Empirical formula	$C_{14}H_{20}N_2O_{15}NiCu$	$C_{14}H_{20}N_2O_{15}CoCu$	$C_{14}H_{20}N_2O_{15}MnCu$
Formula weight	578.57	578.79	574.80
Crystal system	Triclinic	Triclinic	Monoclinic
Space group	$P\bar{1}$	$P\bar{1}$	$P2_1/c$
Unit cell dimensions: (Å, °)			
a	8.273(4)	8.336(3)	8.4433(2)
b	9.667(5)	9.657(3)	26.8632(8)
c	13.842(7)	13.873(4)	9.7817(3)
α	100.99(4)	101.31(2)	90
β	101.81(4)	102.52(3)	97.756(2)
γ	96.96(4)	96.64(2)	90
Temperature (K)	158(2)	158(2)	158(2)
Wavelength (Å)	0.71073	0.71073	0.71073
Volume (Å^3)	1048.8(9)	1054.4(6)	2198.33(11)
Z	2	2	4
μ (mm^{-1})	1.993	1.876	1.619
Density (calculated) (g cm^{-3})	1.832	1.823	1.737
F(000)	590	588	1168
Crystal size (mm)	0.5 × 0.2 × 0.15	0.3 × 0.3 × 0.04	0.60 × 0.50 × 0.27
Data collection			
Absorption correction	Empirical	Empirical(refdelf)	None
θ range (°)	2.18–24.00	2.18–22.50	1.52–34.92
Reflections collected	3446	3215	45020
Independent reflections	3283 [R(int) = 0.0581]	2738 [R(int) = 0.0608]	8959 [R(int) = 0.0234]
Completeness to $\theta = 24.00°$	99.7%	99.5%	93.0%
Max., min. transmission	0.4182, 0.3739	0.6742, 0.2636	1.000, 0.8156
Range h, k, l	$-9 \le h \le 0$ $-10 \le k \le 10$ $-15 \le l \le 15$	$-8 \le h \le 1$ $-10 \le k \le 10$ $-14 \le l \le 14$	$-12 \le h \le 13$ $-40 \le k \le 43$ $-15 \le l \le 14$
Refinement			
Refinement method	Full-matrix least-squares on $F2$		
Data/restraints/parameters	3283/0/341	2738/36/341	8959/0/342
Goodness-of-fit on F_2	1.034	0.831	1.264
Final R indices [$I > 2\sigma(I)$]			
R_1	0.0482	0.0640	0.0269
wR_2	0.1045	0.1231	0.0741
R indices (all data)			
R_1	0.0791	0.1394	0.0298
wR_2	0.1175	0.1429	0.0803
Largest difference peak and hole (e Å^{-3})	1.401 and −0.417	1.655 and −0.499	0.663 and −0.420

differing only in the presence of a non-stoichiometric water molecule present in the crystal lattices of **1** (0.2 water) and **2** (0.3 water). Figure 1 shows the molecular unit of **1**, figure 2 shows the molecular unit of **2**, and figure 3 shows the molecular unit of **3**; due to the low occupancy of the fractional water molecules, they were not included in final refinements.

All three compounds have very similar bond lengths and angles in the Cu coordination sphere with two of the Cu–O bonds (Cu–O(1) and Cu–O(2)) longer than the other pair of Cu–O bonds by approximately 0.2 Å. This lengthening of the bonds is attributed to the Jahn–Teller effect and indicates that the Cu-equatorial plane

Table 2. Selected bond lengths (Å) and angles (°) for compounds **1–3**.

	1	**2**	**3**
Cu–N(1)	1.977(5)	1.950(9)	1.9751(10)
Cu–N(11)	1.910(5)	1.912(9)	1.9222(10)
Cu–O(1)	2.302(4)	2.295(8)	2.3089(9)
Cu–O(2)	2.337(4)	2.317(7)	2.2755(9)
Cu–O(11)	2.105(4)	2.096(8)	2.1195(9)
Cu–O(12)	2.076(4)	2.075(8)	2.0763(9)
M–O(4)	2.028(4)	2.083(8)	2.1571(9)
M–O(21)	2.044(5)	2.162(8)	2.1468(10)
M–O(22)	2.035(5)	2.065(9)	2.1822(9)
M–O(23)	2.115(5)	2.029(8)	2.2765(9)
M–O(24)	2.020(5)	2.054(8)	2.1439(10)
M–O(25)	2.041(5)	2.082(8)	2.1560(9)
N(1)–Cu–N(11)	178.7(2)	179.1(4)	174.77(4)
N(1)–Cu–O(1)	76.03(18)	75.5(3)	75.39(4)
N(1)–Cu–O(2)	75.79(18)	75.9(3)	77.09(4)
N(1)–Cu–O(11)	101.18(18)	101.8(3)	101.20(4)
N(1)–Cu–O(12)	100.53(19)	101.3(4)	101.04(4)
N(11)–Cu–O(1)	102.63(19)	103.6(3)	109.84(4)
N(11)–Cu–O(2)	105.54(18)	105.0(3)	97.69(4)
N(11)–Cu–O(11)	79.00(19)	78.4(4)	78.63(4)
N(11)–Cu–O(12)	79.22(19)	78.5(4)	79.62(4)
O(1)–Cu–O(2)	151.62(15)	151.1(3)	152.03(3)
O(1)–Cu–O(11)	96.20(17)	96.8(3)	96.01(4)
O(1)–Cu–O(12)	86.23(18)	85.9(3)	85.55(4)
O(2)–Cu–O(11)	92.46(16)	92.9(3)	94.10(4)
O(2)–Cu–O(12)	95.64(18)	95.8(3)	94.91(4)
O(11)–Cu–O(12)	158.10(16)	156.7(3)	157.37(4)
O(4)–M–O(21)	89.32(19)	94.7(3)	88.31(4)
O(4)–M–O(22)	92.46(18)	91.6(3)	88.53(4)
O(4)–M–O(23)	93.82(19)	87.8(3)	95.52(4)
O(4)–M–O(24)	83.86(19)	82.9(3)	80.81(4)
O(4)–M–O(25)	175.10(18)	174.0(3)	170.33(4)
O(21)–M–O(22)	88.8(2)	90.4(3)	88.68(4)
O(21)–M–O(23)	176.7(2)	177.2(3)	175.09(4)
O(21)–M–O(24)	91.6(2)	85.6(3)	97.91(5)
O(21)–M–O(25)	90.5(2)	86.2(3)	90.71(4)
O(22)–M–O(23)	92.22(19)	90.7(4)	88.35(3)
O(22)–M–O(24)	176.30(19)	173.0(3)	167.25(4)
O(22)–M–O(25)	92.43(19)	94.3(3)	101.06(4)
O(23)–M–O(24)	87.7(2)	93.5(4)	85.77(4)
O(23)–M–O(25)	86.3(2)	91.2(3)	86.03(3)
O(24)–M–O(25)	91.3(2)	91.2(3)	89.81(4)

comprises the two pyridine nitrogen atoms and the carboxylate oxygen atoms from the non-bridging pdc. It should be noted that in **3**, the Cu–O(2) bond distance is shorter that the Cu–O(1) bond distance, opposite that seen in **1** and **2**. The lengths of these bonds are also significantly shorter in **3** than in **1** and **2**.

The Cu–pdc bond lengths are between 0.04–0.1 Å shorter than those seen in the analogous $[Cu(H_2O)_5][Cu(pdc)_2] \cdot 2H_2O$ homodimer [5], with the exception of the Jahn–Teller bonds, which are approximately 0.1 Å larger in **1**, **2**, and **3**. Increased lattice constraints due to fractional waters in **1** and **2** and the larger Mn(II) ion in **3** may account for these differences, in addition to the effect of the lower temperature at which measurements were made on **1**–**3**. The Cu–N bond lengths are similar to those reported

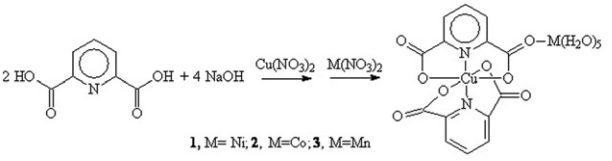

Scheme 1. Preparation of Compounds **1–3**.

for the triclinic $P\bar{1}$ form of the $[Cu(pdc)(H_2O)_2]$ monomer [8a], but the Cu–O bond lengths for **1–3** are in general longer than those reported for all forms of the monomer [8], with the exception of the Cu–O(6) bond in the monoclinic form [8b].

The M–O bond lengths increase with increasing ionic radius of the metal center as expected. One M–O bond to the solvent waters is significantly longer than the others, as also seen in the Cu [5], Ni [6], and Mn homodimers [7]. The Ni–O bond lengths in **1** are all approximately 0.01 Å shorter than those seen in the analogous $[Ni(H_2O)_5][Ni(pdc)_2] \cdot 2H_2O$ homodimer, but are in many cases within the sum of the standard deviations [6]; the remaining differences are easily accounted for by the difference in data collection temperatures. The Co–O bond lengths in **2** are comparable to those in the analogous Co homodimer $[Co(H_2O)_5][Co(pdc)_2] \cdot 2H_2O$ [17]. The Mn–O bond lengths in **3** are approximately 0.09 Å longer than those in the analogous Mn homodimer [7]. This may be caused by changes in bond angles at the chelate metal position (2–6°) resulting from the replacement of one Mn(II) with the smaller Cu(II). Bond angles within the molecular unit are generally within the standard deviation in **1**, **2**, and **3**, with the exception of the N(11)–Cu–O(2) angle which is ~7° narrower in **3** relative to **1** and **2**, and the N(11)–Cu–O(1) angle which is ~6° wider in **3** compared to **1** and **2**. The N(11)–Cu–N(1) bond angle is also smaller by about 5° in **3**.

Compounds **1–3** all undergo extensive hydrogen bonding. A list of hydrogen bonds is given in the supplementary materials. The exact parameters of the hydrogen bonding vary in each compound, but all form extended 3-D networks. Figure 4 shows the hydrogen bonding in **3** along the *b*-axis, while figure 5 shows the bonding along the *a*-axis.

3.2. *UV-Vis characterization*

Aqueous solutions of 2.0 mM $[Cu(H_2O)_6](NO_3)_2$, 2.2 mM $[Co(H_2O)_6](NO_3)_2$, 2.2 mM $[Ni(H_2O)_6](NO_3)_2$, 0.20 mM $Na_2Cu(pdc)_2$, 0.44 mM $Na_2Co(pdc)_2$, 0.44 mM $Na_2Ni(pdc)_2$, 3.4 mM **1**, 3.8 mM **2**, and 0.5 mM **3** were prepared and their UV-Vis spectra were recorded from 400–900 nm (300–900nm for $[Ni(H_2O)_6](NO_3)_2$). A plot of the spectra of $[Cu(H_2O)_6]^{2+}$, $Cu(pdc)_2^{2-}$, **1**, **2**, and **3** is given in figure 6, and a plot of the spectra of $[Ni(H_2O)_6]^{2+}$, $Ni(pdc)_2^{2-}$, $[Co(H_2O)_6]^{2+}$, and $Co(pdc)_2^{2-}$ is given in figure 7. A high concentration of the pdc^{2-} anion was used in each case to favor formation of the bis complex and reduce the likelihood of residual free $M(H_2O)_n$ species in the solution. $Cu(pdc)(H_2O)_2$ has a significantly lower solubility and precipitated from the reaction mixture at low concentrations of pdc^{2-}.

As can be seen in figure 6 the spectra of $Cu(H_2O)_6$ and $Cu(pdc)_2$ are quite similar, with the hexaaqua species exhibiting a broad maximum at ~804 nm and an extinction coefficient of 15 $M^{-1}\,cm^{-1}$, and the *bis*(pdc) species showing a broad maximum at

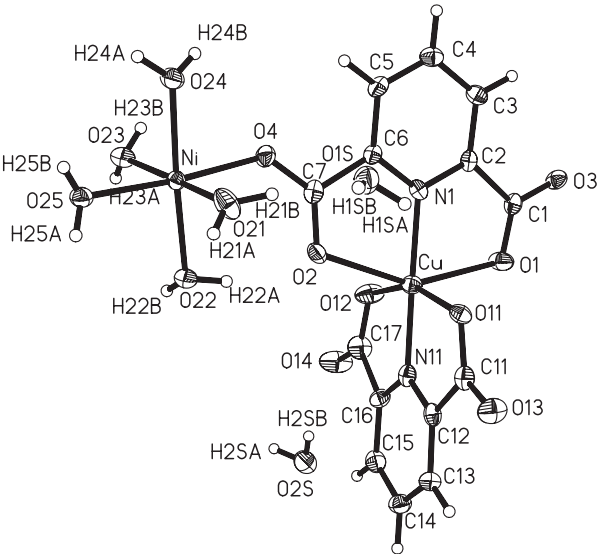

Figure 1. Thermal ellipsoid plot of the molecular unit of **1** showing 50% probability ellipsoids. Only hydrogen atoms involved in hydrogen bonding are labeled.

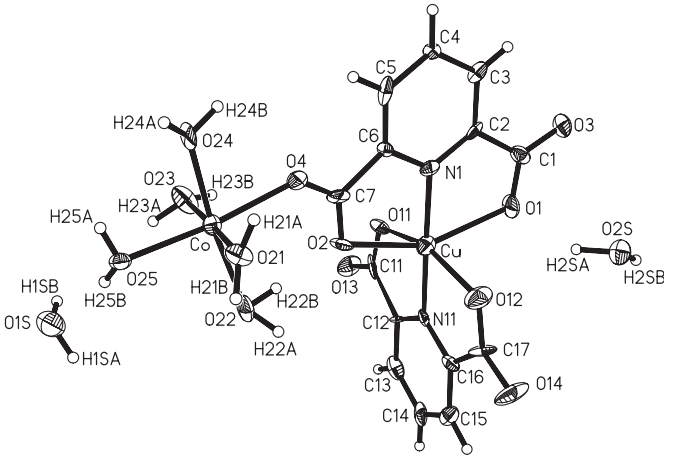

Figure 2. Thermal ellipsoid plot of the molecular unit of **2** showing 50% probability ellipsoids. Only hydrogen atoms involved in hydrogen bonding are labeled.

~774 nm with an extinction coefficient of 67 $M^{-1}\,cm^{-1}$. The main distinguishing feature between the two species is the large difference in their molar extinction coefficients, with the *bis*(pdc) species absorbing approximately four times more strongly than the hexaaqua species.

The data for the Ni and Co species are similar to that for the Cu species in that the *bis*(pdc) species have much larger extinction coefficients than the hexaaqua species. A large shift in the position of the maximum absorbance for each of the compounds is observed after addition of the pdc^{2-}. The $[Co(H_2O)_6]^{2+}$ shows a maximum absorption at ~510 nm with a shoulder at ~480 nm, while the $Co(pdc)_2^{2-}$ moiety has its maximum

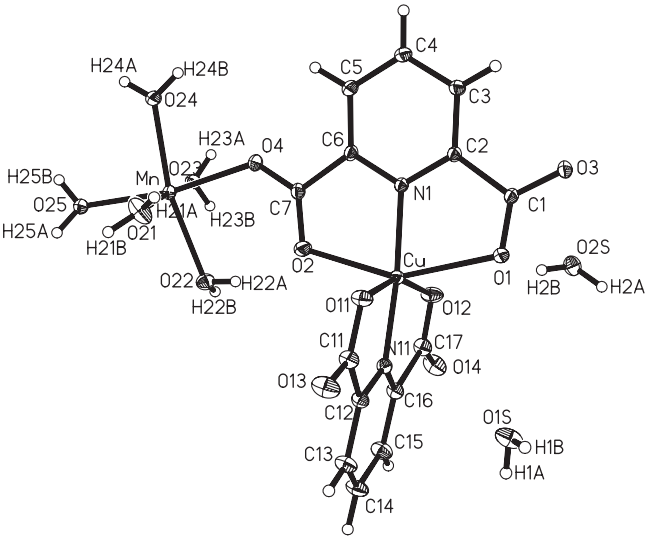

Figure 3. Thermal ellipsoid plot of the molecular unit of **3** showing 50% probability ellipsoids. Only hydrogen atoms involved in hydrogen bonding are labeled.

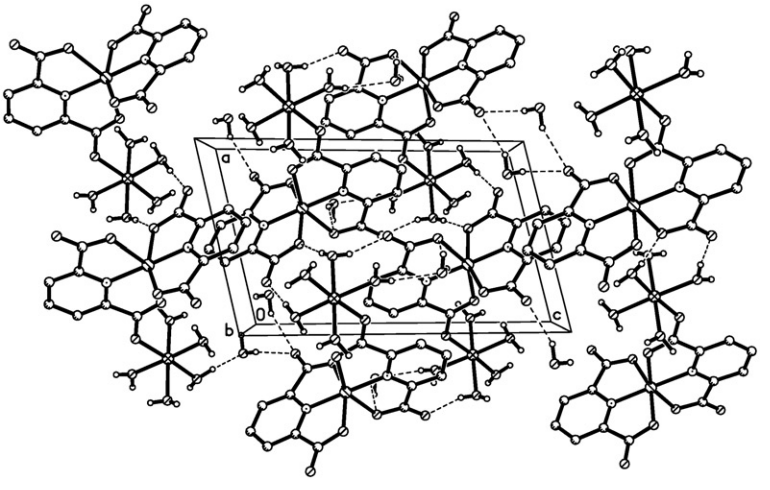

Figure 4. Packing structure of **3** as viewed parallel to the *b*-axis. Hydrogen bonds are shown as dotted lines.

absorption at ~590 nm. The $[Ni(H_2O)_6]^{2+}$ has two distinct peaks, one at ~390 nm and a split broad peak at ~650 and 730 nm with a shoulder at ~660 nm, while the $Ni(pdc)_2^{2-}$ solution has only one peak at ~605 nm. The large absorbance in the spectra below 450 nm is believed to be due to the pdc ligand.

The solutions of **1** and **3** show only one peak in the visible spectra around 775 nm and extinction coefficients between 65 and 70 $M^{-1}cm^{-1}$ (see the Experimental section for exact values). The position of the maximum and significant increase in the molar extinction coefficients strongly suggests that the Cu(II) ions in solution are bound by the pdc ligands. The solution of **2** shows two peaks, one near 775 nm with a molar

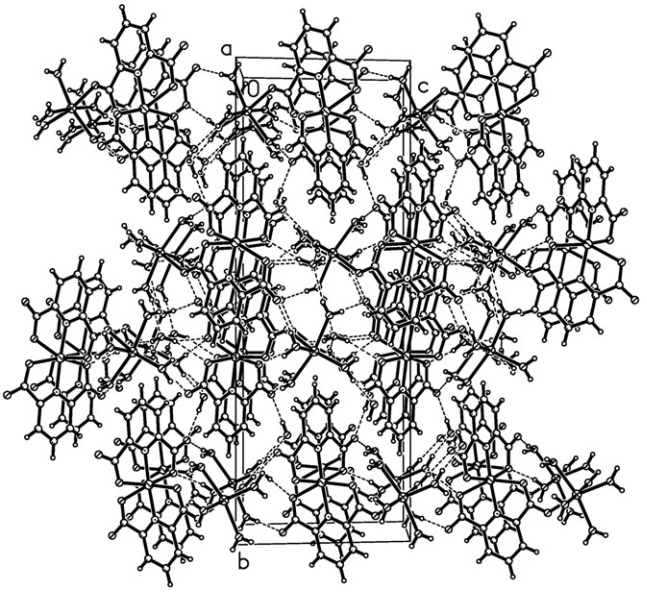

Figure 5. Packing structure of **3** as viewed parallel to the *a*-axis. Hydrogen bonds are shown as dotted lines.

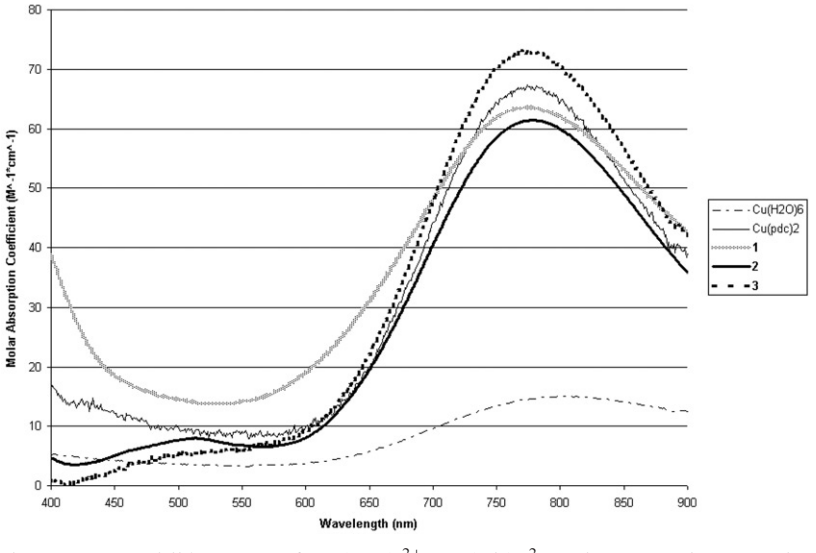

Figure 6. UV-Visible spectra of $[Cu(H_2O)]^{2+}$, $[Cu(pdc)_2]^{2-}$ and compounds **1**, **2**, and **3**.

extinction coefficient of approximately $60\,M^{-1}\,cm^{-1}$, consistent with that of the $Cu(pdc)_2^{2-}$ ion, and another around 515 nm with a molar extinction coefficient of approximately $8\,M^{-1}\,cm^{-1}$ consistent with that of the $[Co(H_2O)_6]^{2+}$ ion, although the molar extinction coefficient is slightly higher than that seen in the pure solution.

It is clear that both $[Ni(pcd)_2]^{2-}$ and $[Co(pdc)_2]^{2-}$ (see figure 7) show significant absorptions near 600nm, which are absent in the spectra of **1** and **2** (see figure 6),

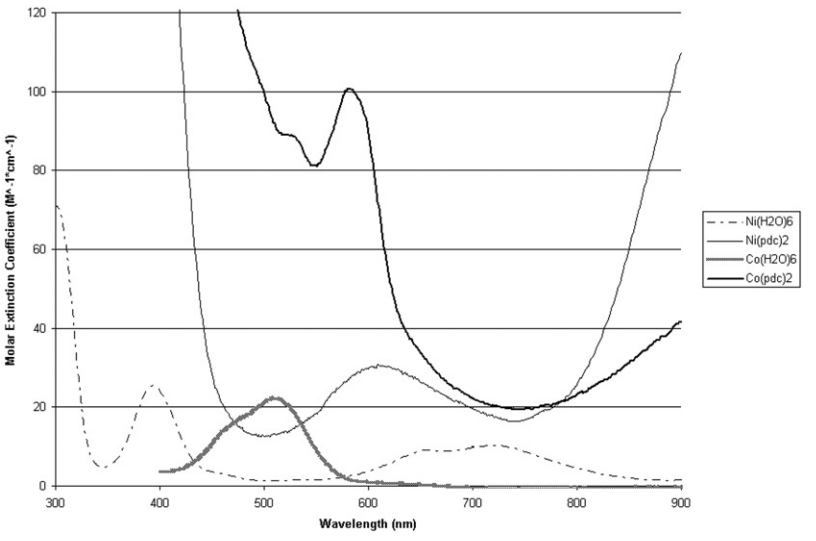

Figure 7. UV-Visible spectra of $[Ni(H_2O)_6]^{2+}$, $[Ni(pdc)_2]^{2-}$, $[Co(H_2O)_6]^{2+}$ and $[Co(pdc)_2]^{2-}$.

suggesting the absence of those species in the mixed complexes. In addition, the absorption due to the aquacobalt specie near 515 nm (figure 7) is clearly visible in the spectrum of the mixed compound **2** (figure 6) The corresponding absorption for the aqua nickel ion is seen as two broad, weak maxima near 650 and 730 nm. These would be too weak to observed under the much stronger signal from the $[Cu(pcd)_2]^{2-}$ ion. While one cannot eliminate the possibility that there is some mixing of metal ions in the different sites, the chelated pdc^{2-} binding pocket is predominantly occupied by the Cu^{2+} ions in the mixed complexes.

3.3. *Magnetic data*

Susceptibility data were collected at 1 kOe from 1.8–325 K for **1**–**3** (figures 8–11) Compound **1** was fit to a model for a Ni–Cu heterodimer [4a] (figure 8), the best fit parameters are given in table 3. Compound **1** exhibits a decrease in the value of χ^*T at low temperatures, decreasing from its maximum value of 1.818 at 325 K to 0.697 at 1.8 K. A Curie–Weiss fit to χ^{-1} gave a Curie constant of 1.79(3) and a θ of $-2.8(2)$ K, with $R^2 = 0.997$. The data showed a good fit to the theoretical model for χ *versus* T, and the presence of a weak antiferromagnetic interaction is confirmed by the decrease in the value of χ^*T at low temperatures. From the fit the exchange strength within the Ni–Cu dimers is $-1.634(8)$ K.

Compound **2** was fit to a model for a mixed Co–Cu heterodimer both with and without contribution from single-ion anisotropy [4b] neither was able to accurately model the observed behavior, however, a plot of the raw data is given in figure 9. The plot of χ^*T (figure 10) shows two distinct downturns, one at ~65 K and a second at ~5 K. It is believed that the first downturn is due to the single-ion anisotropy of the Co(II) ion, and the second is caused by a three dimensional ordering transition at low temperatures, although data below 1.8 K would be required to confirm the presence

of three dimensional ordering. The value of χ^*T decreases from its maximum of 3.88 at 325 K to 1.72 at 1.8 K, and appears to be approaching the origin (figure 10). A Curie-Weiss fit for **2** was not attempted due to the single-ion anisotropy of the Co(II) ion.

Compound **3** was fit to a model for a mixed Mn–Cu heterodimer without contribution from single-ion anisotropy, the best fit values are given in table 3 [4b] (figure 11). A small decrease in the value of χ^*T from 4.91 at 325 K to 3.91 at 1.8 K occurs in **3**. A Curie–Weiss fit to χ^{-1} gave values of 4.86(3) for the Curie constant and −0.67(6) for θ with $R^2 = 0.99996$, in excellent agreement with the fit to χ *versus* T. These data are consistent with the presence of very weak antiferromagnetic interactions on the order of −0.37 K within the Mn–Cu dimers.

4. Discussion

Heterobimetallic complexes provide a challenge for analysis with respect to the location of the individual metal ions. A recent article [10] which reported the synthesis of compounds **1** and **2** in this work, suggested that the Ni(II) or Co(II) ions occupied the chelating site in the pdc ligands and that the Cu(II) was found in the aqua site, coordinated to the pdc only through the bridging carboxylate. This result was based upon the observation that all the Cu(II) containing bimetallic complexes studied exhibited a broad absorption at ca 780 nm. This seemed counterintuitive to us in light of the known preference of Cu(II) for N-based ligands. UV-Visible spectroscopy of $Cu(NO_3)_2$ and comparison with the spectrum of $Cu(pdc)_2^{2-}$ shows that even at high concentrations of pdc^{-2} (9 equivalents), the Cu(II) d–d transition shifts only 20 nm, from ~800 nm to ~780 nm, with an accompanying 4-fold increase in the extinction coefficient, clearly indicating the coordination of the pdc anions to the Cu(II) ions,

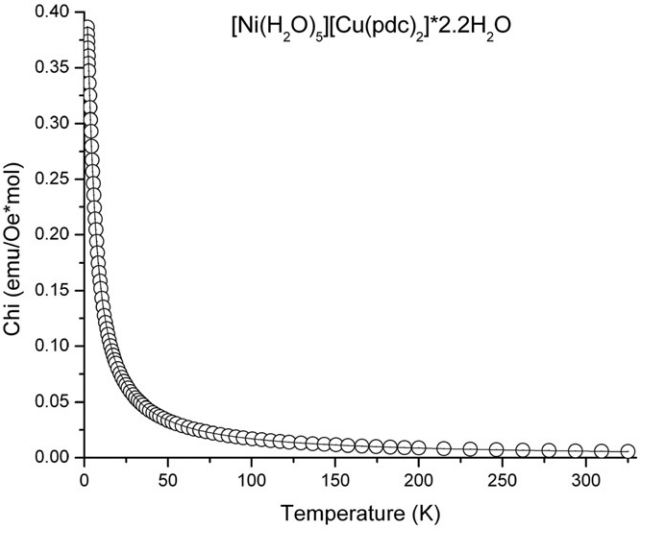

Figure 8. Magnetic susceptibility as a function of temperature for **1** in a 1.0 kOe field. The solid line represents the best fit to the model for a $S = 1/2, 3/2$ heterodimer.

whereas coordination of either Ni(II) or Co(II) to the pdc anion under the same conditions shows much more significant shifts in the UV-Visible spectrum. As such, we do not believe that the presence of a broad feature near 800 nm is a useful diagnostic for the location of the Cu(II) ion.

Additional evidence for the location of the Cu ion in the chelating site comes from the X-ray structures of **1**–**3**. We re-refined the structures after switching the locations of the two metal ions (that is, placing the Cu(II) ion in the aqua site and the alternate M^{2+} ion

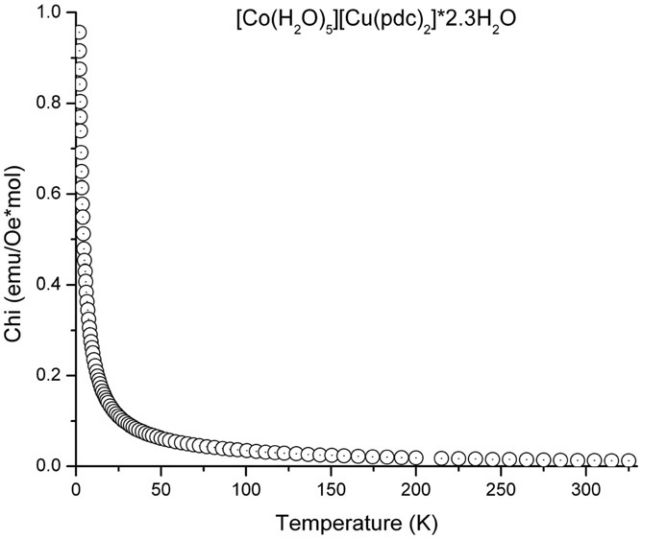

Figure 9. Magnetic susceptibility as a function of temperature for **2** in a 1.0 kOe field.

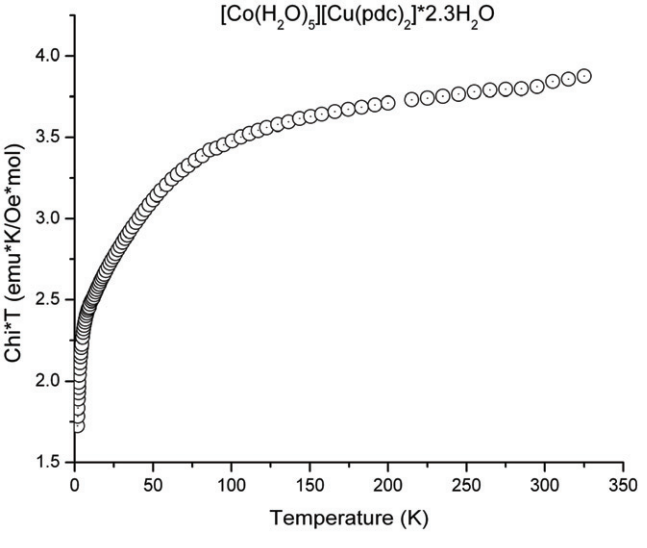

Figure 10. Magnetic susceptibility multiplied by temperature as a function of temperature for **2** in a 1.0 kOe field.

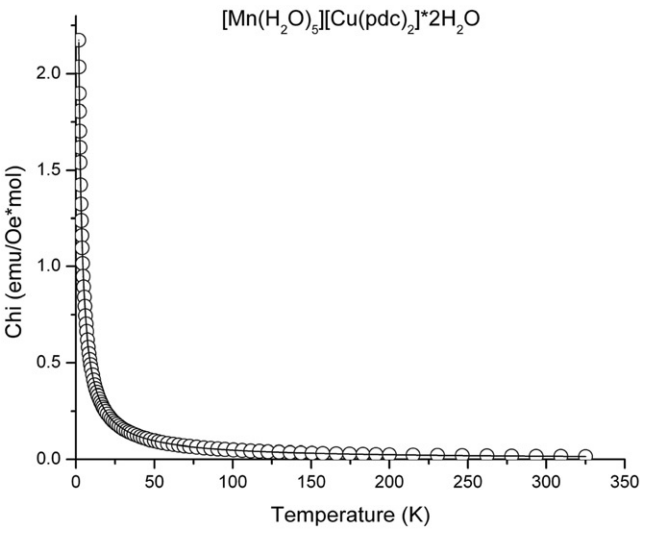

Figure 11. Magnetic susceptibility as a function of temperature for **3** in a 1.0 kOe field. The solid line represents the best fit to the model for a S = 1/2, 5/2 heterodimer.

Table 3. Magnetic fitting parameters for **1** and **3**.

Compound	C	$2J/k$ (K)	R^2
1	1.877(2)	−1.634(8)	0.99997
3	4.832(6)	−0.369(3)	0.99997

in the chelating site). In all cases, the final refined R_1-value increased (with a substantial difference for **3** due to the large difference in electron density between the two metal ions) [$\Delta R_1 = 0.28$ (**1**), 0.41(**2**), 6.12 (**3**)]. In addition, neglecting the fractional occupancy water molecule in **1** and **2**, the largest residual peak occurred near the M atom and the largest residual hole occurred near the Cu ion in the final refinement when the positions were inverted (indicating the deficiency and excess of electron density respectively), while the largest peaks and holes occurred in random locations when the structures were refined with the metal ions in the correct positions. From these combined observations, we are confident that in compounds **1**–**3**, the Cu(II) ion predominantly resides in the chelating site of the pdc ligand and it is the M ion that occupies the aqua site, although we cannot exclude the possibility that there is some randomness.

The magnetic data show weak exchange between the Cu and M′ ions for **1** and **3** ($2J/k = -1.634$ and -0.369 respectively). The coordination mode of the bridging carboxylate in all three compounds is syn-anti (**1**: $\angle_{\text{Ni–O4-C7-O2}} = 12.4°$, $\angle_{\text{Cu–O2-C7-O4}} = 172.0°$; **2** $\angle_{\text{Co-O4-C7-O2}} = 8.2°$, $\angle_{\text{Cu–O2-C7-O4}} = 175.0$; $\angle_{\text{Mn–O4-C7-O2}} = 11.8°$, $\angle_{\text{Cu–O2-C7-O4}} = 11.8$). Theoretical work by Alemany and co-workers [18] suggested that such a superexchange pathway should lead to weak to moderate ferromagnetic interactions in dicopper(II) species, which has been supported by numerous experimental studies on syn-anti carboxylate bridged copper(II) systems [19]. However, weak antiferromagnetic coupling in similar systems has also been reported [20]. In all cases, the exchange observed is weak to moderate with the sign and magnitude affected by the competition

between the ferromagnetic and antiferromagnetic contributions to the exchange [19d, 21]. The current observation of weak antiferromagnetic exchange is in good accord with the reported values. For compound **2** the single ion anisotropy of the Co(II) ion overwhelms the observed temperature dependence of the susceptibility. Attempts to fit the data to the heterodimer model gave ambiguous results and no significant interpretation is made. Historically, attempts to model the magnetic behavior of Co(II) have proven only partially successful [4, 22].

Acknowledgments

We are grateful for grants from the NSF (IMR-0314773) toward the purchase of the MPMS SQUID, from PCISynthesis Inc. toward the purchase of the D8 Powder X-ray Diffractometer, and the Kresge Foundation toward the purchase of both. ARP is grateful for a James and Ada Bickman Summer Science Internship and a Gustav H. Carlson Summer Research Fellowship.

References

[1] (a) L. Li, M.M. Turnbull, C.P. Landee, B. Twamley. *J. Coord. Chem.*, **59**, 1311 (2006); (b) A. Shapiro, C.P. Landee, M.M. Turnbull, J. Jornet, M. Deumal, J.J. Novoa, M. Robb, W. Lewis. *J. Am. Chem. Soc.*, **129**, 952 (2007); (c) A.R. Parent, C.P. Landee, M.M. Turnbull. *Inorg. Chim. Acta*, **360**, 1143 (2007); (d) R.T. Schneider, C.P. Landee, M.M. Turnbull, F.F. Awwadi, B. Twamley. *Polyhedron*, **26**, 1849 (2007); (e) F.M. Woodward, P.J. Gibson, G.B. Jameson, C.P. Landee, M.M. Turnbull, R.D. Willett. *Inorg. Chem.*, **46**, 4256 (2007).
[2] (a) A. Tomkiewicz, J. Mroziński, I. Brüdgam, H. Hartl. *Eur. J. Inorg. Chem.*, 1787 (2005); (b) E. Pardo, R. Ruiz-Garcia, F. Lloret, J. Faus, M. Julve, Y. Journaux, M.A. Novak, F.S. Delgado, C. Ruiz-Perez. *Chem. Eur. J.*, **13**, 2054 (2007); (c) Y. Pei, O. Kahn, J. Sletten, J. Renard, R. Georges, J. Gianduzzo, J. Curely, Q. Xu. *Inorg. Chem.*, **27**, 47 (1988).
[3] H.O. Stumpf, Y. Pei, C. Michaut, O. Kahn, J.P. Renard, L. Ouahab. *Chem. Mater.*, **6**, 257 (1994).
[4] (a) H. Okawa, Y. Imada, M. Tanaka. *Inorg. Chim. Acta*, **129**, 173 (1987); (b) D. Liao, S. Juan, Z. Jiang, S. Yan, P. Cheng, G. Wang. *Polyhedron*, **11**, 2621 (1992).
[5] L. Wang, L. Duan, D. Xiao, E. Wang, C. Hu. *J. Coord. Chem.*, **57**, 1079 (2004).
[6] Y. Wen, Z. Li, Y. Qin, Y. Chen, J. Cheng, Y. Yao. *Acta Cryst.*, **E58**, m762 (2002).
[7] Y. Liu, J. Dou, D. Wang, X. Zhang, L. Zhou. *Acta Cryst.*, **E62**, m2526 (2006).
[8] (a) E.E. Sileo, G. Rigotti, B.E. Rivero, M.A. Blesa. *J. Phys. Chem. Solics*, **58**, 1127 (1997); (b) M. Biagini Cingi, A. Chilsi Villa, C. Guastini, M. Nardelli. *Gazz. Chim. Ital.*, **101**, 825 (1971); (c) M. Koman, J. Moncol, D. Hudecova, B. Dudova, M. Melnik, M. Korabik, J. Mrozinski. *Polish J. Chem.*, **75**, 957 (2001).
[9] (a) G. Nardin, L. Randaccio, R.P. Bonomo, E. Rizzarelli. *J.C.S. Dalton*, **7**, 369 (1980); (b) E.E. Sileo, M.A. Blesa, G. Rigotti, B.E. Rivero, E.E. Castellano. *Polyhedron*, **15**, 4531 (1996); (c) S.K. Ghosh, J. Ribas, P.K. Bharadwaj. *Cryst. Eng. Comm.*, **6**, 250 (2004).
[10] M.V. Kirillova, M.F.C. Guedes da Silva, A.M. Kirillov, J.J.R. Frausto da Silva, A.J.R. Pombeiro. *Inorg. Chim. Acta*, **360**, 506 (2007).
[11] SHELXTL/PC, (version 5.1) Siemens Analytical Instruments Inc. madison, WI 1998.
[12] Siemans (1996). *SMART and SAINT. Area Detector Control, Integration Software*, Siemans Analytical X-ray Instruments, Inc., Madison, WI, USA (1996).
[13] G.M. Sheldrick. *SADABS. Program for Empirical Absorption Correction of Area Detector Data*, University of Göttingen, Germany (1996).
[14] G.M. Sheldrick. *SHELX97-2. Programs for the Solution, Refinement of Crystal Structures*, University of Göttingen, Germany (1997).
[15] J.A. Ibers, W.C. Hamilton, Eds. *International Tables for Crystallography*, Vol. C, Kynoch Press, Birmingham (1992).
[16] The structures have been deposited with the CCDC. Ref. numbers: **1**, 648495; **2**, 648496; **3**, 648497.

[17] L. Yang, D.C. Crans, S.M. Miller, A. la Cour, O.P. Anderson, P.M. Kaszynski, M.E. Godzala III, L.D. Austin, G.R. Wilsky. *Inorg. Chem.*, **41**, 4859 (2002).
[18] A. Rodríguez-Fortea, P. Alemany, S. Alvarez, E. Ruiz. *Chemistry-E.J.*, **7**, 627 (2001).
[19] (a) E. Colacio, J.M. Domínguez-Vera, R. Kivekäs, J.M. Moreno, A. Romeroa, J. Ruiz. *Inorg. Chim. Acta*, **212**, 115(1993); (b) S. Sen, M.K. Saha, T. Gupta, A.K. Karmakar, P. Kundu, S. Mitra, M.B. Hursthouse, K.M.A. Malik. *J. Chem. Cryst.*, **28**, 771-7 (1998); (c) B. Zurowska, J. Mroziński. *Inorg. Chim. Acta*, **342**, 23 (2003); (d) E. Colacio, J.M. Dominquez-Vera, J. Manuel, J.P. Costes, R. Kivekäs, J.P. Laurent, J. Ruiz. *Inorg. Chem.*, **31**, 774 (1992); (e) E. Colacio, J.-M. Domínguez-Vera, R. Kivekäs, J. Ruiz. *Inorg. Chim. Acta*, **218**, 109 (1994); (f) L.-J. Zhou, X.-J. Luan, Y.-Y. Wang, G.-H. Lee, Q.-Z. Shi, S.-M. Peng. *J. Coord. Chem.*, **59**, 1107 (2006).
[20] (a) P.K. Coughlin, S.J. Lippard. *J. Am. Chem. Soc.*, **106**, 2328 (1984); (b) E. Colacio, J.P.Costes, R. Kivekäs, J.P. Laurent, J. Ruiz, M. Sundberg. *Inorg. Chem.*, **30**, 1475 (1991).
[21] E. Colacio, J.P. Costes, R. Kivekäs, J.P. Laurent, J. Ruiz. *Inorg. Chem.*, **29**, 4240 (1990).
[22] (a) A. Gulbrandsen, J. Sletten, K. Nakatani, Y. Pei, O. Kahn. *Inorg. Chim. Acta*, **212**, 271 (1993); (b) N. Duran, W. Clegg, L. Cucurull-Sanchez, R.A. Coxall, H.R. Jimenez, J. Moratal, F. Lloret, P. Gonzalez-Duarte. *Inorg. Chem.*, **39**, 4821 (2000).